Proceedings of Meetings on Acoustics

Volume 19, 2013 http://acousticalsociety.org/

ICA 2013 Montreal
Montreal, Canada
2 - 7 June 2013

Noise
Session 3aNSb: Aviaton, Aviation Engines, and Flow Noise

3aNSb5. Autocorrelation analysis of military jet aircraft noise

Blaine Harker*, Kent L. Gee, Tracianne B. Neilsen, Alan T. Wall, Sally A. McInerny and Michael M. James

***Corresponding author's address: Department of Physics and Astronomy, Brigham Young University, N283 ESC, Provo, UT 84602, blaineharker@gmail.com**

Jet noise research has seen increased use of autocorrelation analyses to glean physical insight about the source and its radiation properties. Length scales and other features have been identified in support of models incorporating large-scale (LSS) and fine-scale (FSS) turbulent structures. In this paper, the meaningful use of autocorrelation in jet noise analysis is further examined. A key finding is that the effect of the peak frequency on autocorrelation width needs to be removed prior to making conclusions about the relative LSS and FSS contributions. In addition, the Hilbert transform is applied to create an envelope of the autocorrelation function to more consistently define a characteristic time scale. These methods are first applied to the analytical LSS and FSS similarity spectra, previously developed by Tam et al. [AIAA 96-1716, 1996]. It is found that the envelope of the FSS similarity autocorrelation function is more similar to that of a delta function than the LSS envelope. These curves are used to more effectively quantify FSS and LSS features in noise spectra from the F-22A Raptor. [Work supported by ONR.]

Published by the Acoustical Society of America through the American Institute of Physics

 [DOI: 10.1121/1.4799991]
Received 11 Dec 2012; published 2 Jun 2013
Proceedings of Meetings on Acoustics, Vol. 19, 040072 (2013)

1. INTRODUCTION

Correlation analysis has been used to study features of jet noise fields for over five decades,[1-3] during which time techniques have been further developed in order to better understand the sources and mechanisms of jet noise radiation. For example, correlation analyses have been used in characterizing equivalent sources,[2, 4-6] to measure sound speed and sound speed gradients[7], to relate flow and acoustic variables,[8-10] and to establish spatial and temporal relationships in the acoustic field at different locations.[1,5] These commonly involve autocorrelation calculations in conjunction with two-point cross-correlations.

In the past few years, usage of the autocorrelation function as a means of providing physical insight of jet noise fields has increased.[3, 11, 12] For example, Tam *et al.*[3] used the autocorrelation of far-field pressure measurements on a heated, supersonic laboratory-scale jet to draw conclusions about the physical size of the "energetic acoustic pulses" radiating from the jet plume, i.e., a correlation length scale. In their paper, they describe various forms of evidence in support of a two-source model of jet noise[13, 14] that consists of large-scale (LSS) and fine-scale (FSS) turbulent structures. In regions to the sideline of a jet, FSS dominates while radiation downstream is primarily attributed to LSS. They showed that the characteristic shape and the width of the autocorrelation changed significantly when comparing sideline measurements to those farther downstream. Because autocorrelation width is proportional to acoustic length scales, they concluded that their autocorrelation analysis supported the two-source model of jet noise.

However, one potential challenge with the use of the autocorrelation function to determine FSS and LSS radiation is its dependence of its width on spectral peak frequency. For jet noise spectra with relatively high peak frequencies, the autocorrelation is naturally narrower than for a spectrum with low frequencies dominating. However, the peak frequency is not the only characteristic of jet noise, so high and low peak frequencies do not uniquely define FSS and LSS radiation across a measurement span for a single jet, nor across jets of different scales or conditions. Thus, it is difficult to ascribe autocorrelation width to the *nature* of the radiation without a form of scaling.

With these difficulties in mind, we approach the use of the autocorrelation for jet noise analysis differently than previous work. In this paper, the influences of the dominant acoustic wavelengths are mitigated by scaling autocorrelation measurements by their respective peak frequencies. In addition, the envelope functions of these non-dimensionalized autocorrelations are calculated via the Hilbert transform. The envelope function allows for a more direct comparison of function widths. These are both discussed in Sec. 2. To provide a physical benchmark, these methods are implemented at the conclusion of Sec. 2 on similarity correlation functions derived from inverse transforming the LSS and FSS similarity spectra defined by Tam *et al.*[13, 14] In Sec. 3., they are used to interpret the nature of the noise radiation from a static F-22A Raptor with one engine at military power.

2. METHODOLOGIES FOR JET NOISE AUTOCORRELATION ANALYSIS

Before moving to jet noise, an overview of autocorrelation is presented, along with emphasis on how the features of the resulting autocorrelation function can be interpreted. Because jet noise may be viewed as band-limited noise, the autocorrelation function for bandpass white noise is examined, which reveals the importance of scaling by the peak frequency and its relation to the correlation length defined by Tam *et al.*[3] The envelope of the autocorrelation function, calculated with the Hilbert transform, provides a more consistent analysis tool for investigating autocorrelation decay rates in jet-noise data. Finally, the autocorrelation and autocorrelation envelopes are given for the LSS and FSS spectra to guide our analysis of the measured data.

2.1 Time-scaled Autocorrelation

The FSS and LSS similarity spectra are indicative of two distinct sources of turbulent mixing noise. As displayed in Figure 1(a), the LSS spectrum is more narrowly shaped and is attributed to Mach-wave radiation that is spatially coherent along the jet axis, whereas FSS radiation has a much broader frequency range and is attributed to the small turbulence fluctuations in the plume.[3] Because the FSS and LSS spectra are shaped broadband spectra, the consideration of rectangular bandpass white noise, which has a convenient analytical autocorrelation function, provides insight into how the autocorrelation of jet noise signals can be interpreted. Specifically, the autocorrelation of rectangular bandpass white noise is related to both bandwidth B and center frequency f_0:[15]

$$R_{xx}(\tau) \propto \mathrm{sinc}(2\pi B\tau)\cos(2\pi f_0\tau). \quad (1)$$

As $B \to 0$, the sinusoidal wave result is recovered: $R_{xx}(\tau) \propto \cos(2\pi f_0\tau)$. On the other hand, as $B \to \infty$, $R_{xx}(\tau)$ approaches a delta function, the white noise autocorrelation. For jet noise, which can be considered a shaped bandpass spectrum, both the spectral width, [similar to B in Eq. (1)] and peak frequency (similar to f_0) are directly related to the autocorrelation.

Because the peak frequency and spectral shape of jet noise vary widely with angle around the jet, a scaled autocorrelation $R_{xx}(\eta)$, where $\eta = \tau \cdot f_{\mathrm{peak}}$, becomes favorable because it removes the dependence of the autocorrelation function on f_{peak} and leaves only the effects of B. Although a given spectral shape may not necessarily be centered about the peak frequency (f_{peak}), it is usually a good approximation and scales $R_{xx}(\tau)$ as desired.

Before continuing, it is important to connect the principle of frequency-scaled autocorrelation to the work of Tam *et al.*[3] Although they did not explicitly investigate the effect of peak frequency on R_{xx}, they recognized the usefulness of quantifying the features of the autocorrelation. They defined a correlation length that is calculated from a time delay corresponding to the maximum anti-correlation in the waveform multiplied by the speed of sound. However, this was only carried out for LSS signals because it appears that a well-defined anti-correlation does not exist for signals dominated by FSS noise. To provide a more consistent analysis technique that can be used for both FSS and LSS-dominated signals, we now investigate an autocorrelation envelope based on the Hilbert transform of the autocorrelation.

2.2 Hilbert Transform and Autocorrelation Envelope

Once the autocorrelation has been time-scaled such that the effect of peak frequency is removed, the features of the scaled autocorrelation function are more clearly related to the shape of the spectrum. The remaining differences in the effective decay of the autocorrelation at different locations of the jet can be quantified with the envelope function:[15]

$$A_{xx}(\eta) = [R_{xx}^2(\eta) + \tilde{R}_{xx}^2(\eta)]^{1/2}, \quad (2)$$

where $\tilde{R}_{xx}(\eta)$ is the Hilbert transform of the autocorrelation. The decay of $A_{xx}(\eta)$ can be measured in order to calculate a characteristic time scale [e.g., $A_{xx}(\eta) = 1/e$] with which to compare $R_{xx}(\eta)$ for different waveforms. The use of frequency-scaled autocorrelation envelopes allows for a clearer comparison of the nature of the radiation at different locations and for different jets than the work done by Tam *et al.*[3] Additionally, since $A_{xx}(\eta)$ is a positive function, it can be plotted on a logarithmic scale to more clearly observe low-amplitude features not visible in $R_{xx}(\eta)$.

2.3 Autocorrelation of FSS and LSS Spectra

As examples of peak-frequency scaled autocorrelation functions and corresponding envelopes, consider the inverse Fourier transforms of the FSS and LSS similarity autospectra,[13, 14] which are shown for the same peak frequency in Figure 1(a). These peak-frequency scaled autocorrelation coefficients, $R_{xx}(\eta)$, have been calculated for the first time and are displayed in Figure 1(b). It is visible that the FSS shape is more similar to the delta-function shape expected for white noise. The autocorrelation of the LSS has greater anti-correlation, with minimum values of the negative loops less than -0.2. Although they never evaluated $R_{xx}(\tau)$ for the LSS, Tam *et al.*[3] cited large negative loops in the correlation as indicative of LSS radiation.

The Hilbert-transform-calculated envelopes of the FSS and LSS autocorrelation functions are also displayed in Figure 1(b). When the $R_{xx}(\tau)$ are scaled by the peak frequency to produce $R_{xx}(\eta)$, the widths of their central peaks are very similar, but slower decay in overall correlation of the LSS (e.g. because of the greater anticorrelation) is easily seen with $A_{xx}(\eta)$. The widths and decay rates are further examined in Figure 1(c), where $10\log_{10}(A_{xx})$ is plotted for FSS and LSS. On this scale, the LSS envelope seems to have a linear decay for at least the first 20 dB down from the peak. When scaled by the peak frequency, comparisons of the FSS and LSS autocorrelations and envelopes to those of jet noise measurements can help produce more quantitative physical insight into the nature of the radiated sound field.

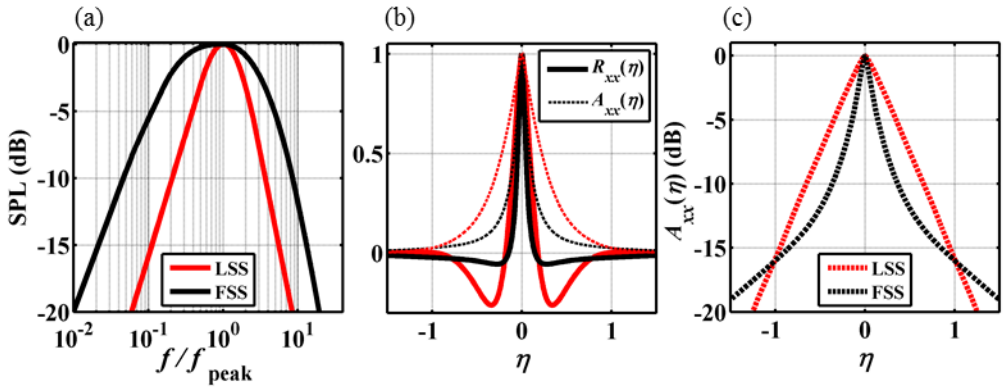

FIGURE 1. (a) One-third octave similarity spectra of the LSS (red) and FSS (black). (b) Peak-frequency scaled autocorrelation coefficient of LSS spectrum (solid red), FSS spectrum (solid black), and their respective envelopes calculated by the Hilbert transform (dashed red and black respectively). (c) Scaled autocorrelation coefficient envelope shown on a decibel scale.

3. APPLICATION OF AUTOCORRELATION ANALYSIS TO FULL-SCALE, HIGH-POWER JET NOISE

Measurements were made of a Pratt and Whitney model F119-PW-100 turbofan engine installed on the Boeing/Lockheed-Martin F-22A Raptor, conducted at Holloman Air Force base [see Figure 2(a)]. One of the engines on the tied-down aircraft was operated at military power while the other was held at idle. An array of 50 GRAS 6.35-mm and 3.18-mm microphones [marked by blue dots on Figure 2(b)] were placed on the ground at a fixed position 11.6 m from the centerline of the jet. For a detailed description of the experiment, see Ref. [16]. Of these sideline locations, two microphones, located at 90° and 130° (measured relative the engine inlet and referenced to 5.5 m downstream) are selected for comparison.

The one-third octave spectra and (un-scaled) autocorrelation coefficient of the 90° and 130° measurements are given in Figure 2(c) and Figure 2(d). In Figure 2(c), the spectrum at 90° is more rounded than at 130°, which is of a more peaked nature. As examined by Neilsen *et al.,*[17] the 90° measurement is at a sideline location where the FSS appears to be the principal contributor to its spectrum. At military power, the 130° measurement is taken in a region where the LSS should dominate. In Figure 2(d), the autocorrelation measurement shows that the autocorrelation width at 90° is much narrower than at 130°. Using the length scale developed by Tam *et al.,*[3] the correlation length at 90° is about 0.5 m while at 130° it is about 1.4 m. However, the peak frequency of each spectrum is different, making it difficult to draw conclusions relating the measurements to additional source characteristics.

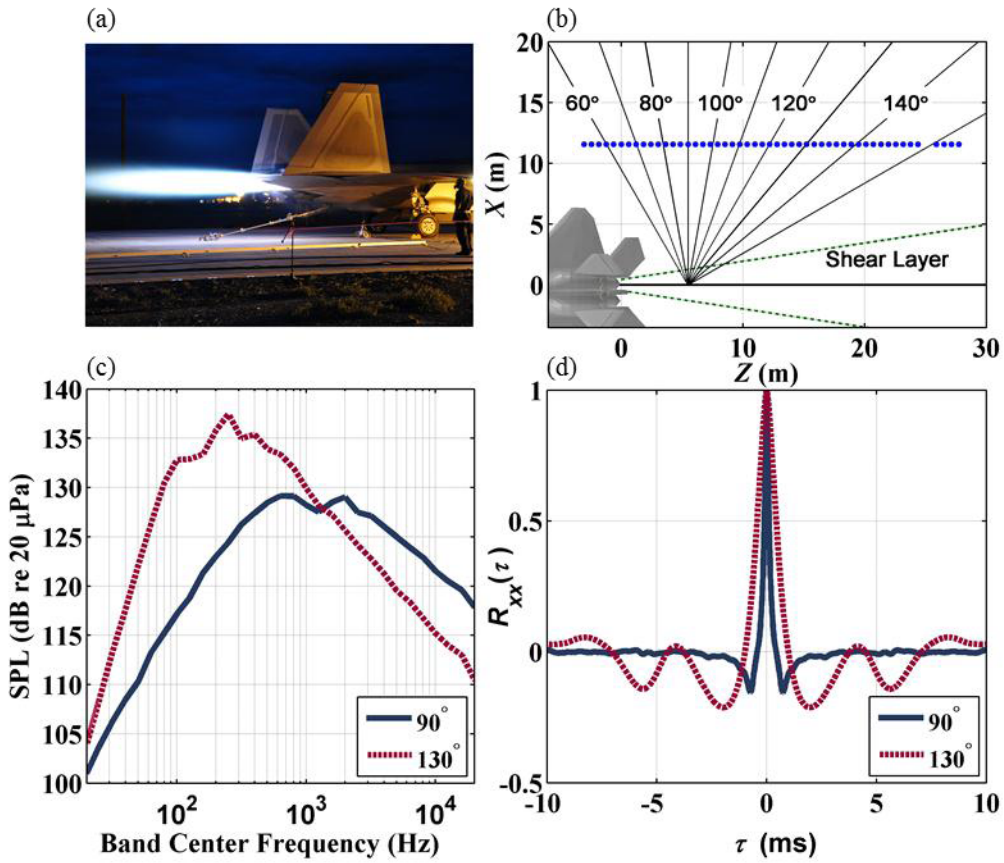

FIGURE 2. (a) Acoustic measurement of an F-22 Raptor at Holloman Air Force base. (b) Measurement schematic of the ground-based array of 50 pressure microphones. Polar angles are measured with respect to the estimated maximum aeroacoustic source region. (c) One-third octave spectra at 90° and 130° positions for a single engine at military power. (d) Autocorrelation coefficient of signals at 90° and 130°.

In Figure 3, we use $R_{xx}(\eta)$ and $A_{xx}(\eta)$ defined for the FSS and LSS spectra to draw conclusions on the type of acoustic radiation at each measurement angle. The one-third octave spectra at 90° and 130° are repeated, referenced to their respective narrowband peak frequencies, in Figure 3(a) and Figure 3(b). Because of the one-third octave processing, the peak in the spectral shapes are not centered at $f/f_{\text{peak}} = 1$. The scaled autocorrelation measurements at 90° and 130° are shown below in Figure 3(c) and Figure 3(d). The distance between the negative loops once scaled are now about 0.5 for both measurement angles, which shows that the length scale developed by Tam *et al.*[3] is directly related to the peak frequency of the spectra. The shape of $R_{xx}(\eta)$ at 90° [in Figure 3(c)] is similar to the FSS autocorrelation from Figure 1(b); however the negative loops indicate that this measurement may have some small combination of the LSS spectra, which is supported by Neilsen *et al.*[17] For the measurement at 130° in Figure 3(d), there are large negative loops in $R_{xx}(\eta)$ indicative of LSS. There are also two pairs of significant negative loops at 130° instead of the one pair seen by Tam *et al.*[3] in the downstream direction. This may be a result of the double-peaked nature of the measured spectrum.

In order to better compare the measured and similarity $A_{xx}(\eta)$, the autocorrelation coefficient envelopes are again plotted on a decibel scale in Figure 3(e) and Figure 3(f). The FSS and LSS scaled envelopes are also plotted to allow for physical insight to be obtained by comparing their respective scaled autocorrelation envelopes. There is general agreement with the envelope of the 90° measurement and the FSS envelope. The negative loops in the autocorrelation coefficient at 90° do not appear to cause a significant deviation from the results for FSS when their respective envelopes are compared, except for a slightly greater measured correlation than predicted at $|\eta| \approx 0.4$. In Figure 3(f), $A_{xx}(\eta)$ is shown for both the LSS and the 130° measurement. The scaled autocorrelation envelope measured at 130° has a linear roll-off that shows agreement with the LSS envelope for the first 10 dB down. However, the second lobe of the measurement's envelope deviates from the LSS envelope. At $\eta = 2$, there is more than an order of magnitude difference between the two envelopes, showing significantly more correlation over time

than what the Tam spectra predict. Therefore, in the maximum radiation region, the characteristics of the jet noise radiation are distinctly different from the LSS. Looking ~30 dB down from the peak, the LSS envelope diverges from a linear roll-off. Although the cause of this is still under investigation, this may be an artifact of the piecewise function used to define the LSS spectra. In summary, comparing the scaled autocorrelation envelopes of the FSS and LSS to those of measured data provide physical insight into the nature of the radiated sound field.

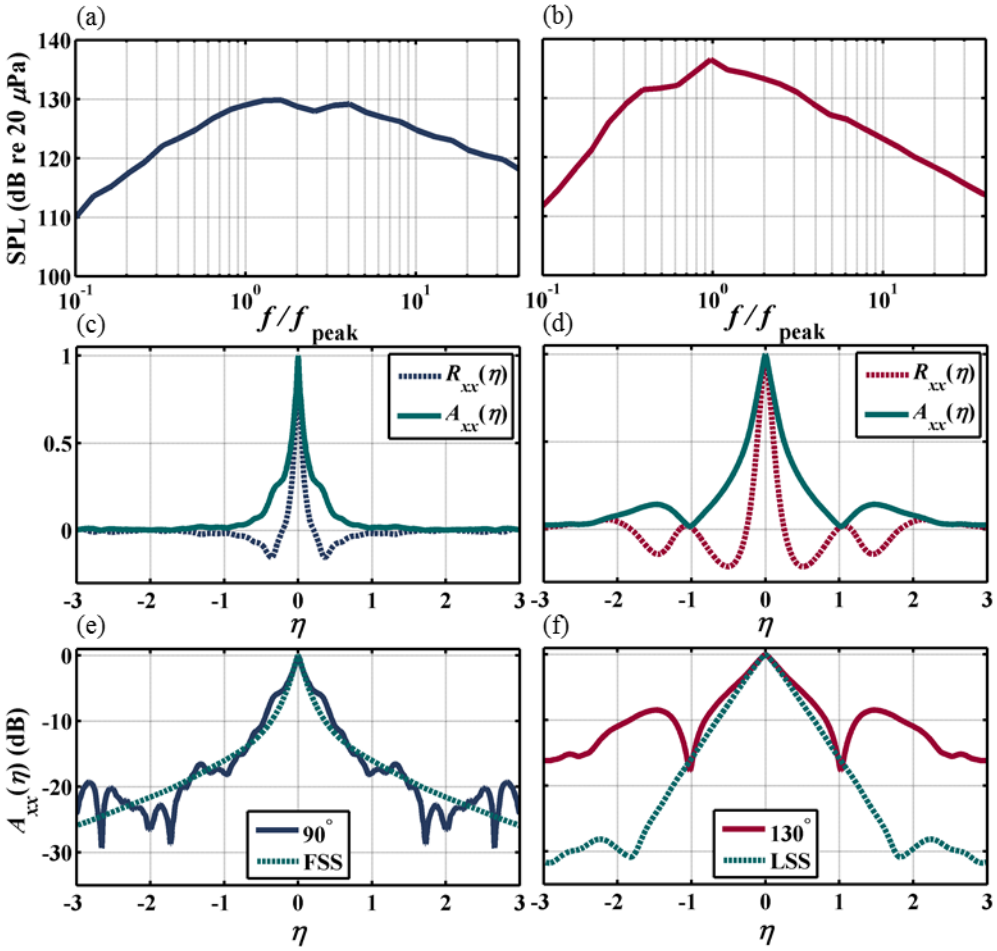

FIGURE 3. One-third octave spectra are shown at (a) 90° and (b) 130° (scaled by the peak frequency). Scaled autocorrelation coefficients and their respective envelopes of (c) the signal at 90°, as well as (d) the signal at 130°. The scaled autocorrelation coefficient envelope is plotted (on a log scale) for (e) the signal at 90° with that of the FSS spectrum, and for (f) the signal at 130° with that of the LSS spectrum.

4. CONCLUSION

In scaling the time scales of autocorrelation measurements by their peak frequency and calculating the Hilbert transform, we have presented a way to examine autocorrelation for deeper physical insight across a jet measurement aperture and across different jet scales. Also, presented for the first time are "similarity autocorrelation functions," by calculating the inverse Fourier transforms of previously developed similarity spectra for large and fine-scale radiation. These analysis techniques and similarity functions have been applied to noise from the F-22A Raptor at sideline and maximum radiation angles. The envelope corresponding to the FSS shows good agreement with the data at the sideline, whereas in the maximum radiation direction the envelope function for the measured data exhibits regions of higher correlation (more than an order of magnitude) than does the predicted envelope function of the LSS.

This paper has focused on developing methods for interpreting jet noise autocorrelation calculations, which have had limited, successful application to full-scale, high-power jet data. These analysis techniques can now be used to

gain further insight at other angles and engine conditions, and for other jet noise measurements. Additionally, although significant progress has been made to relate the autocorrelation measurements to the nature of the sound field radiation, the manner in which the acoustic length scales relating these envelopes ties to the turbulent source length scales needs to be the subject of further investigations.

ACKNOWLEDGMENTS

The authors gratefully acknowledge funding for this analysis from the Office of Naval Research. The measurements were funded by the Air Force Research Laboratory through the SBIR program and supported through a Cooperative Research and Development Agreement (CRADA) between Blue Ridge Research and Consulting, Brigham Young University, and the Air Force. The authors also recognize the contributions of Dan Santos with the 508 ASW/YF at Hill Air Force Base and Senior Master Sergeant Neil Raben and the 49th Fighter Wing at Holloman Air Force Base in completing the experiment.

SBIR DATA RIGHTS - (DFARS 252.227-7018 (JUNE 1995)); Contract Number: FA8650-08-C-6843; Contractor Name and Address: Blue Ridge Research and Consulting, LLC, 15 W Walnut St. Suite C; Asheville, NC Expiration of SBIR Data Rights Period: March 17, 2016 (Subject to SBA SBIR Directive of September 24, 2002). The Government's rights to use, modify, reproduce, release, perform, display, or disclose technical data or computer software marked with this legend are restricted during the period shown as provided in paragraph (b)(4) of the Rights in Noncommercial Technical Data and Computer Software—Small Business Innovation Research (SBIR) Program clause contained in the above identified contract. No restrictions apply after the expiration date shown above. Any reproduction of technical data, computer software, or portions thereof marked with this legend must also reproduce the markings.

Distribution A – Approved for Public Release; Distribution is Unlimited 88ABW-2012-6367.

REFERENCES

1. B. L. Clarkson, "Correlation of pressures around a jet engine," Proceedings of WADC University of Minnesota Conference on Acoustical Fatigue, WADC TR 59-676 (Mar. 1961), pp. 85-98.
2. H. V. Fuchs, "Space correlations of the fluctuating pressure in subsonic turbulent jets," J. Sound Vib. **23**, 77-99 (1972).
3. C. K. W. Tam, K. Viswanathan, K. K. Ahuja, and J. Panda, "The sources of jet noise: Experimental evidence," J. Fluid Mech. **615**, 253-292 (2008).
4. H. V. Fuchs, "Application of acoustic mirror, telescope and polar correlation techniques to jet noise source location," J. Sound Vib. **58**, 117-126 (1978).
5. K. Viswanathan, J. R. Underbrink, and L. Brusniak, "Space-time correlation measurements in near fields of jets," AIAA J. **49**, 1577-1599 (2011).
6. M. J. Fisher, M. Harper-Bourne, and S. A. L. Glegg, "Jet engine noise source location: The polar correlation technique," J. Sound Vib. **51**, 23-54 (1977).
7. W. J. Baars, C. E. Tinney, N. E. Murray, B. J. Jansen, and P. Panickar, "The effect of heat on turbulent mixing noise in supersonic jets," AIAA Paper 2011-1029, (2011).
8. J. Panda, R. G. Seasholtz, and K. A. Elam, "Investigation of noise sources in high-speed jets via correlation measurements," J. Fluid Mech. **537**, 349-385 (2005).
9. J. Panda and R. G. Seasholtz, "Experimental investigation of density fluctuations in high-speed jets and correlation with generated noise," J. Fluid Mech. **450**, 97-130 (2002).
10. M. J. Doty and D. K. McLaughlin, "Space–time correlation measurements of high-speed axisymmetric jets using optical deflectometry," Exp. Fluids **38**, 415-425 (2005).
11. P. J. Morris and K. B. M. Q. Zaman, "Velocity measurements in jets with application to noise source modeling," J. Sound Vib. **329**, 394-414 (2010).
12. S. Karabasov, M. Afsar, T. Hynes, A. Dowling, W. McMullan, C. Pokora, G. Page, and J. McGuirk, "Jet noise: Acoustic analogy informed by large eddy simulation," AIAA J. **48**, 1312-1325 (2010).
13. C. K. W. Tam, M. Golebiowski, and J. M. Seiner, "On the two components of turbulent mixing noise from supersonic jets," AIAA Paper 96-1716, (1996).
14. C. K. W. Tam and K. B. M. Q. Zaman, "Subsonic jet noise from nonaxisymmetric and tabbed nozzles," AIAA J. **38**, 592-599 (2000).
15. J. S. Bendat and A. G. Piersol, *Random Data: Analysis and Measurement Procedures*, 4th ed. (John Wiley & Sons, Hoboken, NJ, 2010), pp. 109-125, 484-486.
16. A. T. Wall, K. L. Gee, M. M. James, K. A. Bradley, S. A. McInerny, and T. B. Neilsen, "Near-field noise measurements of a high-performance military jet aircraft," Noise Control Eng. J. **60**, 421-434 (2012).
17. T. B. Neilsen, K. L. Gee, A. T. Wall, and M. M. James, "Similarity spectra analysis of high-performance jet aircraft noise," J. Acoust. Soc. Am. (submitted 2012).